sensor. Each estimate made use of a group of measurements (typically twenty or more) that together overconstrained the solution.

This *multiple constraint* method had several drawbacks. First, it had a significantly lower estimate rate due to the need to collect multiple measurements per estimate. Second, the system of nonlinear equations did not account for the fact that the sensor fixture continued to move throughout the collection of the sequence of measurements. Instead, the method effectively assumes that the measurements were taken simultaneously. The violation of this simultaneity assumption could introduce significant error during even moderate motion. Finally, the method provided no means to identify or handle unusually noisy individual measurements. Thus, a single erroneous measurement could cause an estimate to jump away from an otherwise smooth track.

In contrast, the approach we use with the new HiBall system produces tracker reports as each new measurement is made, rather than waiting to form a complete collection of observations. Because single measurements underconstrain the mathematical solution, we refer to the approach as *single-constraint-at-a-time* (*SCAAT*) tracking (Welch, 1996; Welch & Bishop, 1997). The key is that the single measurements provide *some* information about the HiBall's state, and thus can be used to incrementally improve a previous estimate. We intentionally fuse each individual "insufficient" measurement immediately as it is obtained. With this approach, we are able to generate estimates more frequently, with less latency, and with improved accuracy, and we are able to estimate the LED positions online concurrently while tracking the HiBall (section 5.4).

We use a Kalman filter (Kalman, 1960) to fuse the measurements into an estimate of the HiBall *state* $\bar{x}$ (the pose of the HiBall). We use the Kalman filter—a minimum-variance stochastic estimator—both because the sensor measurement noise and the typical user-motion dynamics can be modeled as normally distributed random processes, and because we want an efficient online method of estimation. A basic introduction to the Kalman filter can be found in chapter 1 of Maybeck (1979), and a more complete introductory discussion can be found in Sorenson (1970), which also contains some interesting historical narrative. More-extensive references can be found in Brown and Hwang (1992), Gelb (1974), Jacobs (1993), Lewis (1986), Maybeck (1979), and Welch and Bishop (1995). Finally, we maintain a Kalman filter Web page (Welch & Bishop, 2000) with introductory, reference, and research material.

The Kalman filter has been used previously to address similar or related problems. See, for example, Azarbayejani and Pentland (1995), Azuma (1995), Emura and Tachi (1994), Fuchs (Foxlin) (1993), Mazuryk and Gervautz (1995), and Van Pabst and Krekel (1993). A relevant example of a Kalman filter used for sensor fusion in a wide-area tracking system is given in Foxlin et al. (1998), which describes a hybrid inertial-acoustic system that is commercially available today (Intersense, 2000).

The SCAAT approach is described in detail by Welch (1996), and Welch and Bishop (1997). Included there is discussion of the benefits of using the approach, as opposed to a multiple-constraint approach such as that by Azuma and Ward (1991). However, one key benefit warrants discussion here. There is a direct relationship between the *complexity* of the estimation algorithm, the corresponding *speed* (execution time per estimation cycle), and the *change* in HiBall pose between estimation cycles (figure 12). As the algorithmic complexity increases, the execution time increases, which allows for significant nonlinear HiBall motion between estimation cycles, which in turn implies the need for a more complex estimation algorithm.

The SCAAT approach, on the other hand, is an attempt to reverse this cycle. Because we intentionally use a single constraint per estimate, the algorithmic complexity is drastically reduced, which reduces the execution time, and hence the amount of motion between estimation cycles. Because the amount of motion is limited, we are able to use a simple dynamic (process) model in the Kalman filter, which further simplifies the computations. In short, the simplicity of the approach means that it can run very fast, which means it can produce estimates very rapidly, with low noise.

The Kalman filter requires both a model of the process dynamics and a model of the relationship between

Figure 12.

the process state and the available measurements. In part due to the simplicity of the SCAAT approach, we are able to use a simple position-velocity (PV) process model (Brown & Hwang, 1992). Consider the simple example state vector $\bar{x}(t) = [x_p(t), x_v(t)]^T$, where the first element $x_p(t)$ is the pose (position or orientation) and the second element $x_v(t)$ is the corresponding velocity; that is, $x_v(t) = (d/dt)\, x_p(t)$. We model the continuous change in the HiBall state with the simple differential equation

$$\frac{d}{dt}\bar{x}(t) = \begin{bmatrix} 0 & 1 \\ 0 & 0 \end{bmatrix}\begin{bmatrix} x_p(t) \\ x_v(t) \end{bmatrix} + \begin{bmatrix} 0 \\ \mu \end{bmatrix} u(t), \qquad (1)$$

where $u(t)$ is a normally distributed white (in the frequency spectrum) scalar noise process, and the scalar μ represents the magnitude or spectral density of the noise. We use a similar model with a distinct noise process for each of the six pose elements. We determine the individual noise magnitudes using an offline simulation of the system and a nonlinear optimization strategy that seeks to minimize the variance between the estimated pose and a known motion path. (See section 6.2.2.). The differential equation (1) represents a continuous integrated random walk, or an integrated Wiener or Brownian-motion process. Specifically, we model each component of the linear and angular HiBall velocities as a random walk, and then use these (assuming constant intermeasurement velocity) to estimate the HiBall pose at time $t + \delta t$ as follows:

$$\bar{x}(t + \delta t) = \begin{bmatrix} 1 & \delta t \\ 0 & 1 \end{bmatrix}\bar{x}(t) \qquad (2)$$

for each of the six pose elements. In addition to a relatively simple process model, the HiBall measurement model is relatively simple. For any ceiling LED (section 4.2) and HiBall view (section 4.1), the 2-D sensor measurement can be modeled as

$$\begin{bmatrix} u \\ v \end{bmatrix} = \begin{bmatrix} c_x/c_z \\ c_y/c_z \end{bmatrix} \qquad (3)$$

where

$$\begin{bmatrix} c_x \\ c_y \\ c_z \end{bmatrix} = VR^T(\bar{l}_{xyz} - \bar{x}_{xyz}), \qquad (4)$$

V is the camera viewing matrix from section 5.1, $\bar{l}_{xyz}$ is the position of the LED in the world, $\bar{x}_{xyz}$ is the position of the HiBall in the world, and R is a rotation matrix corresponding to the orientation of the HiBall in the world. In practice, we maintain the orientation of the HiBall as a combination of a global (external to the state) quaternion and a set of incremental angles as described by Welch (1996) and Welch and Bishop (1997).

Because the measurement model (3) and (4) is nonlinear, we use an extended Kalman filter, making use of the Jacobian of the nonlinear HiBall measurement model to transform the covariance of the Kalman filter. Although this approach does not preserve the presumed Gaussian nature of the process, it has been used successfully in countless applications since the introduction of the (linear) Kalman filter. Based on observations of the statistics of the HiBall filter residuals, the approach also appears to work well for the HiBall. In fact, it is reasonable to expect that it would, as the speed of the SCAAT approach minimizes the distance (in state space) over which we use the Jacobian-based linear approximation. This is another example of the importance of the relationship shown in figure 12.

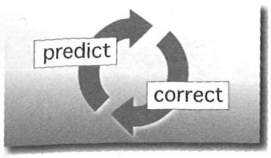

Figure 12a.

At each estimation cycle, the next of the 26 possible views is chosen randomly. Four points corresponding to the corners of the LEPD sensor associated with that view are projected into the world using the 3×4 viewing matrix for that view, along with the current estimates of the HiBall pose. This projection, which is the inverse of the measurement relationship described above, results in four rays extending from the sensor into the world. The intersection of these rays and the approximate plane of the ceiling determines a 2-D bounding box on the ceiling, within which are the candidate LEDs for the current view. One of the candidate LEDs is then chosen in a least-recently-used fashion to ensure a diversity of constraints.

Once a particular view and LED have been chosen in this fashion, the CIB (section 4.3) is instructed to flash the LED and take a measurement as described in section 5.2. This single measurement is compared with a prediction obtained using equation (3), and the difference (or *residual*) is used to update the filter state and covariance matrices using the Kalman gain matrix. The Kalman gain is computed as a combination of the current filter covariance, the measurement noise variance (section 6.2.1), and the Jacobian of the measurement model. This recursive prediction-correction cycle continues in an ongoing fashion, a single constraint at a time.

A more detailed discussion of the HiBall Kalman filter and the SCAAT approach is beyond the scope of this paper. For additional information see Welch (1996) and Welch and Bishop (1997).

5.4 Online LED Autocalibration

Along with the benefit of simplicity and speed, the SCAAT approach offers the additional capability of being able to estimate the 3-D positions of the LEDs in the world concurrently with the pose of the HiBall, online, in real time. This capability is a tremendous benefit in terms of the accuracy and noise characteristics of the estimates. Accurate LED position estimates are so important that, prior to the introduction of the SCAAT approach, a specialized offline approach was developed to address the problem (Gottschalk & Hughes, 1993).

The method we now use for autocalibration involves defining a distinct SCAAT Kalman filter for each LED. Specifically, for each LED, we maintain a state $\bar{l}$ (estimate of the 3-D position) and a 3×3 Kalman filter covariance. At the beginning of each estimation cycle, we form an augmented state vector $\hat{x}$ using the appropriate LED state and the current HiBall state: $\hat{x} = [\bar{x}^T, \bar{l}^T]^T$. Similarly, we augment the Kalman filter error covariance matrix with that of the LED filter. We then follow the normal steps outlined in section 5.3, with the result being that the LED portion of the filter state and covariance is updated in accordance with the measurement residual. At the end of the cycle, we extract the LED portions of the state and covariance from the augmented filter, and save them externally. The effect is that, as the system is being used, it continually refines its estimates of the LED positions, thereby continually improving its estimates of the HiBall pose. Again, for additional information, see Welch (1996) and Welch and Bishop (1997).

5.5 Initialization and Reacquisition

The recursive nature of the Kalman filter (section 5.3) requires that the filter be initialized with a known state and corresponding covariance before steady-state operation can begin. Such an initialization (or *acquisition*) must take place prior to any tracking session, but also upon the (rare) occasion when the filter diverges and "loses lock" as a result of blocked sensor views, for example.

The acquisition process is complicated by the fact that each LEPD sees a number of different widely separated views (section 4.1). Therefore, detecting an LED provides at best an ambiguous set of potential LED directions in HiBall coordinates. Moreover, before acquisition,

no assumptions can be made to limit the search space of visible LEDs. As such, a relatively slow brute-force algorithm is used to acquire lock.

We begin with an exhaustive LED scan of sufficiently fine granularity to ensure that the central primary field of view is not missed. For the present ceiling, we flash every thirteenth LED in sequence, and look for it with the central LEPD until we get a hit. Then, a sufficiently large patch of LEDs, centered on the hit, is sampled to ensure that several of the views of the central LEPD will be hit. The fields of view are disambiguated by using the initial hits to estimate the yaw of the HiBall (rotation about vertical); finally, more-selective measurements are used to refine the acquisition estimate sufficiently to switch into tracking mode.

6 Results

Three days after the individual pieces of hardware were shown to be functioning properly, we demonstrated a complete working system. After months of subsequent tuning and optimization, the system continues to perform both qualitatively and quantitatively as well—or, in some respects, better—than we had anticipated (section 6.1). The articulation of this success is not meant to be self-congratulatory, but to give credit to the extensive and careful modeling and simulation performed prior to assembly (section 6.2). In fact, the Kalman filter parameters found by the optimization procedure described in section 6.2.2 were, and continue to be, used directly in the working system. Likewise, much of the software written for the original simulations continues to be used in the working system.

6.1 Online Operation

The HiBall system is in daily use as a tool for education and research. For example, it was used by Martin Usoh et al. to perform virtual reality experiments comparing virtual "flying," walking in place, and real walking (Usoh et al., 1999). (See figure 13.) The researchers used the HiBall system to demonstrate that, as a mode of locomotion, real walking is simpler, more straightforward, and more natural, than both virtual flying and walking in place. The unprecedented combination of large working volume and the high performance of the HiBall system led the researchers to claim that there was nowhere else that they could have meaningfully performed the experiments.

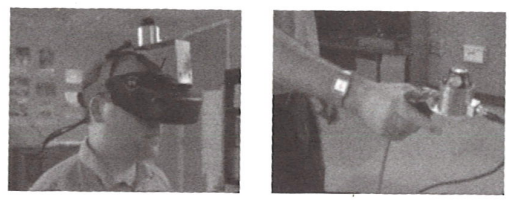

Figure 13.

6.1.1 Robustness. As a result of a mechanical design tradeoff, each sensor field of view is less than six degrees. The focal length is set by the size of the sensor housing, which is set by the diameter of the sensors themselves. Energetics is also a factor, limiting how small the lenses can be while maintaining sufficient light-collecting area. As a result of these design tradeoffs, even a momentary small error in the HiBall pose estimate can cause the recursive estimates to diverge and the system to lose lock after only a few LED sightings. And yet the system is quite robust. In practice, users can jump around, crawl on the floor, lean over, even wave their hands in front of the sensors, and the system does not lose lock. During one session, we were using the HiBall as a 3-D digitization probe, a HiBall on the end of a pencil-shaped fiberglass wand (figure 14, left). We laid the probe down on a table at one point, and were amazed to later notice that it was still tracking, even though it was observing only three or four LEDs near the edge of the ceiling. We picked up the probe and continued using it, without it ever losing lock.

6.1.2 Estimate Noise. The simplest quantitative measurement of estimate noise is the standard deviation of the estimates when a HiBall is held stationary. With a tracker as sensitive as the HiBall, it is important to be certain that it really is stationary. The raised floor in our

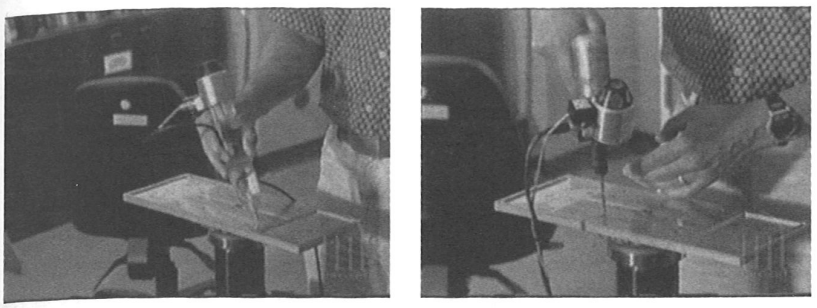

Figure 14.

laboratory allows motion, for example when a person walks by, that is larger than the expected error in the HiBall. We made careful measurements by resting the support for the HiBall on the concrete subfloor in our laboratory. The standard deviation of the HiBall estimates while stationary was approximately 0.2 mm and 0.03 deg. The distribution of the noise fit a normal distribution quite well.

To make measurements of the noise when the HiBall is in motion, we rely on the assumption that almost all of the signal resulting from normal human motion is at frequencies below 2 Hz. We use a high-pass filter (Welch, 1967) on the pose estimates, and assume the output is noise. The resulting statistics are comparable to those made with the HiBall stationary, except at poses for which there are very few LEDs visible in only one or two views. In these poses, near the edge of the ceiling, the geometry of the constraints results in amplification of errors. For nearly all of the working volume of the tracker, the standard deviation of the noise on measurements while the HiBall is still or moving is about 0.2 mm and 0.03 deg.

6.1.3 Absolute Accuracy. We have performed several experiments to measure the accuracy of the HiBall system; however, the most objective experiment took place in July of 1999. Boeing Phantom Works scientists David Himmel and David Princehouse (Associate Technical Fellows) visited our laboratory for two days to assess the accuracy of the HiBall system and its potential use in providing assembly workers with real-time feedback on the pose of handheld pneumatic drills during the aircraft manufacturing process. (The right image in figure 14 shows the HiBall attached to a pneumatic drill.)

The scientists designed some controlled experiments to assess the accuracy of the HiBall system. They brought with them an aluminum "coupon" (see figure 14 and figure 15) with 27 shallow holes drilled on 1.5-in. centers using a numerically controlled milling machine with a stated accuracy of 1/1000 in. The holes (except one) were not actually drilled through the coupon, but instead formed conical dimples with a fine point at the center. The center-most hole (hole 14) was actually drilled completely through to provide a mounting point. Using that hole, we attached the coupon to a military-grade tripod situated on the (false) floor of our laboratory, under the HiBall ceiling. As shown in the left image of figure 14, we mounted the HiBall on our standard probe, a rigid plastic, pencil-like object with a pointed steel tip. We used one of the coupon holes to perform our normal HiBall probe calibration procedure, which involves placing the tip of the probe in the hole, pivoting the probe about the point while collecting several seconds of pose data, and then estimating the transformation from the HiBall to the probe tip. (We have a standard application that assists us with this procedure.) Together with Himmel and Princehouse, we performed several experiments in which we placed the tip of the HiBall probe in each hole in succession, sampling the HiBall pose estimates only when we pressed the probe button. We performed several such sessions over the

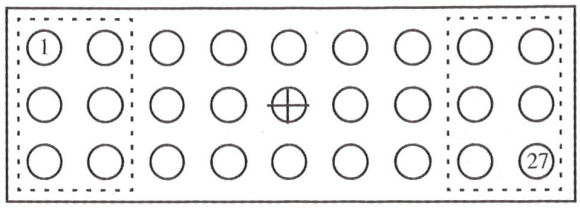

Figure 15.

course of one afternoon and the next morning. (We recalibrated the probe in the morning.)

For the data from each session, we used a least-squares optimization method to find an estimate of the full 6-D transformation (translation and rotation) that minimized the Euclidian distance from the probe data to a 2-D plane with 27 holes on 1.5-in. spacing. The resulting fit consistently corresponded to an average positioning error of 20/1000 in. (0.5 mm) at the metal tip of the HiBall probe, which is within the target Boeing specifications. The system might actually be more accurate than our experiments indicated. For one, the diameter of the (rounded) tip of the HiBall probe is 0.5 mm. In addition, at the time of the experiments, we unfortunately did not heed our own advice to position the experimental platform on the rigid concrete subfloor. In any case, we are encouraged by the results, and are excited about the possibility that the HiBall system has uses beyond tracking for virtual reality.

6.2 Offline Simulation and Modeling

During the design of the HiBall system, we made substantial use of simulation, in some domains to a very detailed level. For example, Zemax (Focus Software, 1995) was used extensively in the design and optimization of the optical design, including the design of the filter glass lenses, and geometry of the optical-component layout. AutoCAD was used to design, specify, and fit check the HiBall body mechanicals, to visualize the physical design, and to transmit the design to our collaborators at the University of Utah for fabrication by the Alpha 1 System (Thomas, 1984; University of Utah Computer Science, 1999). A custom ray-tracing system was built by Stefan Gottschalk (UNC) for the purpose of evaluating the optical behavior and energetics of the primary, secondary, and tertiary fields of view; the results were used by the noise model developed by Chi (1995) as described in section 6.2.1.

In addition, a complete simulator of the system was written in C++. This simulator, discussed further in section 6.2.2, was used to evaluate the speed, accuracy, and robustness of the system. In addition, it was used to "tune" the Kalman filter for realistic motion dynamics. This simulator continues to be used to evaluate mechanical, optical, and algorithmic alternatives.

6.2.1 HiBall Measurement Noise Model. Signal-to-noise performance is a prime determiner of both accuracy and speed of the system, so an in-depth study (Chi, 1995) was performed to develop a detailed noise model accounting for properties of the LED, the LEPD (sensor), the optical system, the physical distance and pose, the electronics, and the dark-light-dark integrations described in section 5.2. The predominant noise source is shot noise, with Johnson noise in the sheet resistivity of the LEPD surfaces being the next most significant. Careful measurements made in the laboratory with the actual devices yielded results that were almost identical to those predicted by the sophisticated model in Chi (1995). A simplified version of this model is used in the real system with the automatic gain control (section 5.2) to predict the measurement noise for the Kalman filter (section 5.3).

6.2.2 Complete System Simulations. To produce realistic data for developing and tuning our algorithms, we collected several motion paths (sequences of pose estimates) from our first-generation electro-optical tracker (figure 3) at its 70 Hz maximum report rate. These paths were recorded from both naive users visiting our monthly "demo days" and from experienced users in our labs. In the same fashion as we had done for Azuma and Bishop (1994a), we filtered the raw path data with a noncausal zero-phase-shift, low-pass filter to eliminate energy above 2 Hz. The output of the low-pass filtering was then resampled at whatever rate we wanted to run the simulated tracker, usually 1,000 Hz.

For the purposes of our simulations, we considered these resampled paths to be the "truth"—a perfect representation of a user's motion. Tracking error was determined by comparing the true path to the estimated path produced by the tracker.

The simulator reads camera models describing the 26 views, the sensor noise parameters, the LED positions and their expected error, and the motion path described above. Before beginning the simulation, the LED positions are perturbed from their ideal positions by adding normally distributed error to each axis. Then, for each simulated cycle of operation, the "true" poses are updated using the input motion path. Next, a view is chosen and a visible LED within that view is selected, and the image-plane coordinates of the LED on the chosen sensor are computed using the camera model for the view and the LED as described in section 5.3. These sensor coordinates are then perturbed based on the sensor noise model (section 6.2.1) using the distance and angle to the LED. These noise-corrupted sensor readings are then fed to the SCAAT filter to produce an updated position estimate. The position estimate is compared to the true position to produce a scalar error metric that is described next.

The error metric we used combines the error in pose in a way that relates to the effects of tracker error on a head-worn display user. We define a set of points arrayed around the user in a fixed configuration. We compute two sets of coordinates for these points: the true position using the true pose and their estimated position using the estimated pose. The error metric is then the sum of the distances between the true and estimated positions of these points. By adjusting the distance of the points from the user, we can control the relative importance of the orientation and the position error in the combined error metric. If the distance is small, then the position error is weighted most heavily; if the distance is large, then the orientation error is weighted most heavily. Our two error metrics for the entire run are the square root of the sum of the squares of all the distances, and the peak distance.

6.2.3 Tuning. Determining the magnitudes of the SCAAT Kalman filter noise parameters (section 5.3) is called *system identification* or *tuning*. We use Powell's method (Press, Teukolsky, Vetterling, & Flannery, 1990) to minimize the error metric described above. Starting with a set of parameters, we run the simulator over a full motion run to determine the total error for the run. The optimizer makes a small adjustment to the parameters and the process is repeated. These runs required hours of computer time and some skill (and luck) in choosing the initial parameters and step sizes. Of course, it is important to choose motion paths that are representative of expected target motion. For example, a run in which the target is very still would result in very different tuning from a run in which the target moves very vigorously.

7 Future Work

7.1 Improving the HiBall

The current SCAAT filter form (section 5.3) and tuning values (section 6.2.3) are a compromise between the responsiveness desired for high dynamics, and the heavy filtering desired for smooth estimates during very slow or no motion. As such, we are investigating the use of a multimodal or multiple-model Kalman filter framework (Bar-Shalom & Li, 1993; Brown & Hwang, 1992). A multiple-model implementation of the HiBall should be able to automatically, continuously, and smoothly choose between one Kalman filter tuned for high dynamics and another tuned for little or no motion. We have this working in simulation, but not yet implemented in the real system.

As mentioned in section 4.3, the system was designed to support wireless communication between the HiBall and the CIB, without significant modification or added information overhead. Despite the fact that commercial head-worn displays are themselves tethered at this time, we are beginning work on a completely wireless HiBall and head-worn display system. We also intend to use the wireless HiBall with projector-based displays where the user is otherwise wearing only polarized glasses. Furthermore, the HiBall was designed with extra built-in digital input-output capabilities. We are considering possibilities for providing access to these signals

for (wireless) user-centered input devices and even body-centric limb tracking.

Finally, we note that a private startup company called 3rdTech (3rdTech, 2000) has negotiated a technology license with UNC for the existing HiBall Tracking System. 3rdTech is now marketing an updated system with simpler LED "strips" instead of ceiling panels.

7.2 Wide-Field-of-View HiBall

Beyond improving the existing system, we continue to head down a path of research and development that will lead to systems with reduced dependency on the laboratory infrastructure. For example, our current ceiling-panel design with 32 LEDs per panel provides far more dense coverage than we believe is necessary. The density of ceiling LEDs is a result of design based on the original sensor fixture shown in figure 3. Given a more sparse field of LEDs, we believe that we could achieve similar performance with a version of the HiBall that has a small number of wide-field-of-view optical sensor units. This would further reduce the packaging size of the user-worn sensor component.

7.3 To the Hallway and Beyond

By leveraging the knowledge gained from successful work in the laboratory, our long-term goal is to achieve similar performance with little or no explicit infrastructure: for example, throughout a building or even (some day) outdoors. Although high-performance 6-D tracking outdoors is a tremendous challenge that is unlikely to be solved any time soon, we believe that the eventual solution will involve a clever and careful combination of multiple complementary technologies. In particular, we are pursuing the hybrid approach initially presented by Welch (1995). We look forward to a day when high-performance 6-D tracking outdoors enables pose-aware devices for work such as Feiner's outdoor augmented reality (Feiner, MacIntyre, Höllerer, & Webster, 1997; Höllerer, Feiner, Terauchi, Rashid, & Hallaway, 1999), the "WorldBoard" initiative (Spohrer, 1999a, 1999b), and other wonderful applications.

Acknowledgments

We acknowledge former Tracker Project members and contributors (alphabetically): Ronald Azuma, Henry Fuchs, Stefan Gottschalk, Pawan Kumar, John Thomas, Jih-Fang Wang, Mark Ward, Scott Williams, Mary Whitton, and Philip Winston. We thank Al Barr (California Institute of Technology) and John "Spike" Hughes (Brown University) for their contributions to the original offline LED calibration work that led to the simpler ceiling panels (figure 1 and figure 10). Finally, we want to acknowledge our many collaborators in the NSF Science and Technology Center for Computer Graphics and Scientific Visualization (below), and in particular our collaborators in mechanical design and fabrication at the University of Utah: Rich Riesenfeld, Sam Drake, and Russ Fish.

This work was supported in part by DARPA/ETO contract DABT 63-93-C-0048 "Enabling Technologies and Application Demonstrations for Synthetic Environments" (Principal Investigators Frederick P. Brooks, Jr. and Henry Fuchs (UNC)), and by the National Science Foundation Cooperative Agreement ASC-8920219 "Science and Technology Center for Computer Graphics and Scientific Visualization," Center Director Rich Riesenfeld (University of Utah) (Principal Investigators Al Barr (Caltech), Don Greenberg (Cornell University), Henry Fuchs (UNC), Rich Riesenfeld, and Andy van Dam (Brown University)).

References

3rdTech. (2000, July 15). *3rdTech™* [Webpage]. Retrieved July 19, 2000, from the World Wide Web: http://www.3rdtech.com/.

Ascension. (2000). *Ascension Technology Corporation* [Webpage]. Retrieved September 15, 2000 from the World Wide Web: http://www.ascension-tech.com/ [2000, September 15].

Azarbayejani, A., & Pentland, A. (1995). Recursive estimation of motion, structure, and focal length. *IEEE Trans. Pattern Analysis and Machine Intelligence, 17*(6), 562–575.

Azuma, R. T. (1993). Tracking requirements for augmented reality. *Communications of the ACM, 36*(July), 50–51.

———. (1995). *Predictive tracking for augmented reality.* Unpublished doctoral dissertation, University of North Carolina at Chapel Hill, Chapel Hill.

Azuma, R. T., & Bishop, G. (1994a). A frequency-domain

analysis of head-motion prediction. *Computer Graphics (SIGGRAPH 94 Conference Proceedings ed.)* (pp. 401–408). Los Angeles: ACM Press, Addison-Wesley.

———. (1994b). Improving static and dynamic registration in an optical see-through hMD. *Computer Graphics (SIGGRAPH 94 Conference Proceedings ed.)* (pp. 197–204). Orlando: ACM Press, Addison-Wesley.

Azuma, R. T., & Ward, M. (1991). *Space-resection by collinearity: Mathematics behind the optical ceiling head-tracker* (Tech. Rep. 91-048). Chapel Hill: University of North Carolina at Chapel Hill.

Bar-Shalom, Y., & Li, X.-R. (1993). *Estimation and Tracking: Principles, Techniques, and Software.* Boston: Artec House, Inc.

Bhatnagar, D. K. (1993). *Position trackers for head mounted display systems: A survey* (Tech. Rep. TR93-010). Chapel Hill: University of North Carolina at Chapel Hill.

Bishop, G. (1984). *The self-tracker: A smart optical sensor on silicon.* Unpublished doctoral Dissertation, University of North Carolina at Chapel Hill, Chapel Hill.

Bishop, G., & Fuchs, H. (1984, January 23–25). *The self-tracker: A smart optical sensor on silicon.* Paper presented at the Advanced Research in VLSI conference, Massachusetts Institute of Technology.

BL. (2000). *CODA mpx30 Motion Capture System [HTML]. B & L Engineering. Retrieved April 27, 2000 from the World Wide Web: http://www.bleng.com/animation/coda/codamain.htm.*

Brown, R. G., & Hwang, P. Y. C. (1992). *Introduction to Random Signals and Applied Kalman Filtering* (2nd ed.). New York: John Wiley & Sons, Inc.

Burdea, G., & Coiffet, P. (1994). *Virtual Reality Technology* (1st ed.). New York: John Wiley & Sons, Inc.

Burton, R. P. (1973). *Real-time measurement of multiple three-dimensional positions.* Unpublished doctoral dissertation, University of Utah, Salt Lake City.

Burton, R. P., & Sutherland, I. E. (1974). Twinkle Box: Three-dimensional computer-input devices. *AFIPS Conference Proceedings, 1974 National Computer Conference, 43,* 513–520.

Chi, V. L. (1995). *Noise model and performance analysis of outward-looking optical trackers using lateral effect photo diodes* (Tech. Rep. TR95-012). Chapel Hill: University of North Carolina at Chapel Hill.

Emura, S., & Tachi, S. (1994). *Sensor fusion based measurement of human head motion.* Paper presented at the 3rd IEEE International Workshop on Robot and Human Communication (RO-MAN 94 NAGOYA), Nagoya University, Nagoya, Japan.

Feiner, S., MacIntyre, B., Höllerer, T., & Webster, A. (1997). A touring machine: Prototyping 3D mobile augmented reality systems for exploring urban environments. *Personal Technologies, 1*(4), 208–217.

Focus Software. (1995). *ZEMAX Optical Design Program User's Guide, Version 4.5.* Tucson, AZ: Focus Software.

Foxlin, E., Harrington, M., & Pfeifer, G. (1998). Constellation™: A wide-range wireless motion-tracking system for augmented reality and virtual set applications. In M. F. Cohen (Ed.), *Computer Graphics (SIGGRAPH 98 Conference Proceedings ed.)* (pp. 371–378). Orlando: ACM Press, Addison-Wesley.

Fuchs (Foxlin), E. (1993). *Inertial head-tracking (manual).* Unpublished master's thesis, Massachusetts Institute of Technology.

Gelb, A. (1974). *Applied Optimal Estimation.* Cambridge, MA: MIT Press.

Gottschalk, S., & Hughes, J. F. (1993). Autocalibration for virtual environments tracking hardware. *Computer Graphics (SIGGRAPH 93 Conference Proceedings ed.)* (pp. 65–72). Anaheim, CA: ACM Press. ACM Press, Addison Wesley.

Höllerer, T., Feiner, S., Terauchi, T., Rashid, G., & Hallaway, D. (1999). Exploring MARS: Developing indoor and outdoor user interfaces to a mobile augmented reality system. *Computers & Graphics, 23,*(6), 779–785.

IGT. (2000). *Image Guided Technologies* [HTML]. Retrieved September 15, 2000 from the World Wide Web: http://www.imageguided.com/.

Intersense. (2000). *Intersense IS-900* [HTML]. Retrieved April 27, 2000 from the World Wide Web: http://www.isense.com/.

Jacobs, O. L. R. (1993). *Introduction to Control Theory* (2nd ed.) New York: Oxford University Press.

Kadaba, M. P., & Stine, R. (2000). *Real-Time Movement Analysis Techniques and Concepts for the New Millennium in Sports Medicine* [HTML]. Motion Analysis Corporation, Santa Rosa, CA. Retrieved September 15, 2000 from the World Wide Web: http://www.motionanalysis.com/applications/movement/rtanalysis.html.

Kalman, R. E. (1960). A new approach to linear filtering and prediction problems. *Transaction of the ASME—Journal of Basic Engineering, 82*(series D), 35–45.

Lewis, F. L. (1986). *Optimal Estimation with an Introductory to Stochastic Control Theory.* New York: John Wiley & Sons, Inc.

MAC. (2000). *HiRes 3D Motion Capture System* [HTML]. Motion Analysis Corporation. Retrieved September 15, 2000 from the World Wide Web: http://www.motionanalysis.com/applications/movement/gait/3d.html.

Maybeck, P. S. (1979). *Stochastic models, estimation, and control* (Vol. 141). New York: Academic Press.

Mazuryk, T., & Gervautz, M. (1995). Two-step prediction and image deflection for exact head tracking in virtual environments. *Proceedings of EUROGRAPHICS 95, 14*(3), 30–41.

Meyer, K., Applewhite, H., & Biocca, F. (1992). A survey of position trackers. *Presence, a publication of the Center for Research in Journalism and Mass Communication, 1*(2), 173–200.

Mulder, A. (1994a). *Human movement tracking technology* (Tech. Rep. TR 94-1). School of Kinesiology, Simon Fraser University.

———. (1994b, May 8, 1998). *Human Movement Tracking Technology: Resources* [HTML]. School of Kinesiology, Simon Fraser University. Retrieved September 15, 2000 from the World Wide Web: http://www.cs.sfu.ca/people/ResearchStaff/amulder/personal/vmi/HMTT.add.html.

———. (1998, May 8, 1998). *Human Movement Tracking Technology* [HTML]. School of Kinesiology, Simon Fraser University. Retrieved September 15, 2000 from the World Wide Web: http://www.cs.sfu.ca/people/ResearchStaff/amulder/personal/vmi/HMTT.pub.html.

Polhemus. (2000). *Polhemus* [HTML]. Retrieved September 15, 2000 from the World Wide Web: http://www.polhemus.com/home.htm.

Press, W. H., Teukolsky, S. A., Vetterling, W. T., & Flannery, B. P. (1990). *Numerical Recipes in C: The Art of Scientific Computing* (2nd ed.). Cambridge University Press.

Sorenson, H. W. (1970). Least-squares estimation: From Gauss to Kalman. *IEEE Spectrum, 7*(July), 63–68.

Spohrer, J. (1999a). Information in places. *IBM Systems Journal, Pervasive Computing, 38*(4).

Spohrer, J. (1999b, June 16). *WorldBoard: What Comes After the WWW?* [HTML]. Learning Communities Group, ATG, Apple Computer, Inc. Retrieved December 24, 1999 from the World Wide Web: http://worldboard.org/pub/spohrer/wbconcept/default.html.

Sutherland, I. E. (1968). A head-mounted three dimensional display. *Proceedings of the 1968 Fall Joint Computer Conference, AFIPS Conference Proceedings* (vol. 33, part 1, pp. 757–764). Washington, D.C.: Thompson Books.

Thomas, S. W. (1984, December). *The Alpha_1 computer-aided geometric design system in the Unix environment.* Paper presented at the Computer Graphics and Unix Workshop.

UNC Tracker Project. (2000, July 10). *Wide-Area Tracking: Navigation Technology for Head-Mounted Displays* [HTML]. Retrieved July 18, 2000 from the World Wide Web: http://www.cs.unc.edu/~tracker.

University of Utah Computer Science. (1999). *Alpha 1 Publications* [HTML]. University of Utah, Department of Computer Science. Retrieved May 28, 1999 from the World Wide Web: http://www.cs.utah.edu/projects/alpha1/a1_publications.html.

Usoh, M., Arthur, K., Whitton, M. C., Bastos, R., Steed, A., Slater, M., & Brooks, F. P., Jr. (1999). Walking > Walking-in-Place > Flying, in Virtual Environments. In A. Rockwood (Ed.), *Computer Graphics (SIGGRAPH 99 Conference Proceedings ed.)* (pp. 359–364). Los Angeles: ACM Press, Addison Wesley.

Van Pabst, J. V. L., & Krekel, P. F. C. (1993, September 20–22). *Multi sensor data fusion of points, line segments and surface segments in 3D space.* Paper presented at the 7th International Conference on Image Analysis and Processing, Capitolo, Monopoli, Italy.

Wang, J.-F. (1990). *A real-time optical 6D tracker for head-mounted display systems.* Unpublished doctoral dissertation, University of North Carolina at Chapel Hill, Chapel Hill.

Wang, J.-F., Azuma, R. T., Bishop, G., Chi, V., Eyles, J., & Fuchs, H. (1990, April 16–20). *Tracking a head-mounted display in a room-sized environment with head-mounted cameras.* Paper presented at the SPIE 1990 Technical Symposium on Optical Engineering and Photonics in Aerospace Sensing, Orlando, FL.

Wang, J.-F., Chi, V., & Fuchs, H. (1990, March 25–28). *A real-time optical 3D Tracker for head-mounted display systems.* Paper presented at the Symposium on Interactive 3D Graphics, Snowbird, UT.

Ward, M., Azuma, R. T., Bennett, R., Gottschalk, S., & Fuchs, H. (1992, March 29–April 1). *A demonstrated optical tracker with scalable work area for head-mounted display systems.* Paper presented at the Symposium on Interactive 3D Graphics, Cambridge, MA.

Welch, G. (1995). *Hybrid self-tracker: An inertial/optical hybrid three-dimensional tracking system* (Tech. Rep. TR95-048). Chapel Hill: University of North Carolina at Chapel Hill, Department of Computer Science.

———. (1996). *SCAAT: Incremental tracking with incomplete information.* Unpublished doctoral dissertation, University of North Carolina at Chapel Hill, Chapel Hill.

Welch, G., & Bishop, G. (1995). *An introduction to the Kalman filter* (Tech. Rep. TR95-041). Chapel Hill: University of North Carolina at Chapel Hill, Department of Computer Science.

———. (1997). SCAAT: Incremental tracking with incomplete information. In T. Whitted (Ed.), *Computer Graphics (SIGGRAPH 97 Conference Proceedings ed.)* (pp. 333–344). Los Angeles: ACM Press, Addison-Wesley.

———. (2000, January 23, 2000). *The Kalman Filter* [HTML]. University of North Carolina at Chapel Hill. Retrieved April 29, 2000 from the World Wide Web: http://www.cs.unc.edu/~welch/kalman/index.html.

Welch, G., Bishop, G., Vicci, L., Brumback, S., Keller, K., & Colucci, D. N. (1999). The HiBall tracker: High-performance wide-area tracking for virtual and augmented environments. *Proceedings of the ACM Symposium on Virtual Reality Software and Technology* (pp. 1–11). University College London, London, United Kingdom (December 20–23): ACM SIGGRAPH, Addison-Wesley.

Welch, P. D. (1967). The use of fast Fourier transform for the estimation of power spectra: A method based on time averaging over short, modified periodograms. *IEEE Transactions on Audio Electroacoust, AU*(15), 70–73.

Woltring, H. J. (1974). New possibilities for human motion studies by real-time light spot position measurement. *Biotelemetry, 1,* 132–146.